Strength and Water Stability of a Fiber-reinforced Cemented Loess

Jun Zhang, Xing-Zhong Weng, Jun-Zhong Liu

Air Force Engineering University, Xi'an, Shaanxi CHINA

Correspondence to:
Jun Zhang email: kgdzjtg@163.com

ABSTRACT

This article discusses the strength and water stability of fiber-reinforced cemented loess (FRCL). The unconfined compressive tests, the anti-erosion tests and the Cantabro tests were performed for soaked and non-soaked specimens. The aforementioned specimens were made by mixing of loess with different cement and fiber ratios. Results indicate that the mixing of cement and fiber significantly improve the strength and the water stability of samples. The unconfined compressive strength (UCS) of samples increases with the increase of cement content. The UCS first increases and thereafter decreases with the increase of fiber content; the optimum content of fiber ranges between 0.3% and 0.45%. The total erosion mass and the erosion rate of samples were decreased by increasing the cement and fiber contents. It is pertinent to note that: (1) the anti-erosion performance of the fiber-reinforced soil was approximately 26-75% higher than that of the cemented soil, and (2) the improvement of UCS was beneficial to the anti-erosion performance. The scattering process of samples can be divided into three stages, i.e., initial stage, rapid-scattering stage and stable stage.

Keywords: Airport engineering, Fiber-reinforced cemented loess, unconfined compressive strength, Anti-erosion test, Cantabro test.

INTRODUCTION

Airstrips can be built to cater the emergency need. In this regard, the construction method and materials, the construction time and the process of soil consolidation for a site-selection play key roles. The stable and reinforced materials may include cement, lime, curing agents and different types of fibers; these materials can be used for many purposes.

During the years 2001 to 2007, the U.S. Army Engineer Research and Development Center developed a program of Joint Rapid Airfield Construction; results of full-scale field tests showed that the fiber reinforced cemented soil could meet the specifications required for a suitable airstrip [1]. Fiber-reinforced soil technology is a new technique to improve the soil, especially when fiber and cement are selected as reinforcing materials. It can replace the requirement of physical reinforcement and enhances the mechanical properties of soil [2]. The existing applications of fiber reinforced soil and fiber reinforced stabilized (e.g. by cement) soil in many areas also indicate the promising prospects of fiber reinforced cemented soil for use in airstrips [3].

Research studies, laboratory tests, field tests and simulations have been carried out to study the mechanical properties of soil, i.e., UCS, tensile and shear strengths of sandy soil, soft soil and expansive soil (either reinforced by natural fiber or synthetic fiber). Divya evaluated the tensile strength-strain characteristics of fiber-reinforced bentonite through a specially developed tensile test [4]. Lecompte [5] and Tang [6] studied the bonding strength between fiber and soil through modified special apparatus; the used fibers were coconut (plant fiber) and polypropylene fiber. Zhu developed a tri-linear model to describe the pullout behavior of short fiber in reinforced soil [7]. Alrashidi carried out many strength tests to study the durability and mechanistic evaluation of soil-cement mixtures reinforced with processed cellulose fibers and polypropylene fibers [8]. Danso added the coconut, bagasse and oil palm fibers in soil building blocks to study the compressive and tensile strength of the blocks [9]. Park measured the strength and ductility characteristic of polyvinyl alcohol fiber reinforced cemented sand [10]. Tang employed a direct method

to measure the tensile strength and anti-crack performance of polypropylene fiber reinforced soil [11]. Akbulut evaluated the use of waste fiber materials such as scrap tire rubber, polyethylene, and polypropylene fiber for the modification of clay soils through unconfined compression, shear box, and resonant frequency tests [12]. Punthutaecha [13], Mohamed [14] and Kumar [15] used polypropylene fiber, nylon fiber, hay fiber, and polyester fiber to restrict the swelling force of expansive soil. Kumar [16] and Ibraim [17] explored the influence fibers with different cross-sections and different lengths. However, few studies have been done so far to determine the water stability of fiber-reinforced cemented loess (FRCL). In fact, the poor water stability of the base course is one of the major reasons for the failure of pavement.

Precipitation can penetrate into the base course from cracks on the surface of pavement, especially during heavy rainfall. The penetrated water may saturate the base course. When aircraft use the runway and taxiway, the load produces large dynamic water pressure on the base course. The dynamic water pressure may cause great damages to the base course [18]. If the base course is damaged, the aircraft cannot operate normally. In order to study the factors influencing anti-erosion performance, Sha [19-20] and Zhu [21] developed a test method and device and pointed out that good anti-erosion performance was essential for semi-rigid base materials. The damage exhibits three aspects- low soaked strength, poor anti-erosion performance and poor anti-scattering performance [22]. Therefore, it is necessary to have good water stability in the base course of pavement.

In this article, the mechanical properties of soil and the performance of water stability of FRCL are investigated under soaked and non-soaked conditions by controlling their cement contents (i.e., 6%, 8% and 10% by weight of dry soil), their fiber contents (i.e., 0.15, 0.3, 0.45, 0.6, 0.8 and 1% by weight of dry soil) and their curing time (i.e., 3d, 7d and 14d). The tests may contain UCS tests, anti-erosion tests in two different ways and the Cantabro test. The water stability of the FRCL, the anti-erosion mechanism and the scattering failure form of FRCL were analyzed.

MATERIALS AND METHODS

Materials

Xi'an soil was selected as an experimental soil. This is representative of northern China. The sample was taken from a construction site in the eastern suburb of Xi'an. This is representative of wet collapsible loess. According to the *Test Methods of Soils for Highway Engineering* (JTG E40-2007), Xi'an soil was classified as a clay soil. *Table I* shows the physical properties of soil sample. The cement used in the experiment was the *Qinling* brand of composite Portland cement (P·C 32.5R). Modified monofilament polypropylene fiber was chosen as a reinforcement material (*Kaitai* brand). The length of the chosen fiber was 12 mm. *Table II* shows the properties of the fiber.

TABLE I. Physical characteristics of soil.

Liquid limit wL/%	Plastic limit wP/%	Plasticity index I_P	Maximum dry density/(g·cm^{-3})	Name of soil
38.2	23.4	14.8	1.89	Silty clay

TABLE II. Material characteristics of differential polypropylene fiber.

Diameter /μm	Fracture strength /Mpa	Initial modulus /Gpa	Density /(g·cm-3)	Elongation at break/%
30	≧400	≧3.5	0.91	15~35

Test Methods

(1) Anti-Erosion Test

Two different methods were adopted by using the shaking table and the fatigue testing machine. The test specimens were formed by using the method of static pressure in accordance with the 95% degree of compaction. The size of specimens was *Φ*100 mm × *H*100 mm. The specimens were submerged for 24 hours before the test. The vibration frequency of the shaking table was 50 Hz and the amplitude ranged between 0.3-0.7mm.

A fatigue testing machine was used to apply the vibration loads for another method. The test apparatus contained three parts- the pressure head, the specimen and the barrel with water. The pressure head can be used to exert adjustable pressures and frequencies. A loading pressure of 0.8 MPa and a loading frequency of 5 Hz were applied. During the test, the pressure head exerted pressure on the specimen through a porous pad of rubber.

The test apparatus can be used to simulate the "pump-absorb action", which was caused by the dynamic water pressure. As shown in *Figure 1*, the "pump-absorb action" can be divided into the following two steps: (i) when the pressure head moved down, pressure is exerted on the rubber pad and the water in the gap of porous rubber pad is quickly squeezed out. The dynamic water pressure formed exerts erosional effects on the surface of specimen, (ii) when the pressure head moves up rapidly, the space between the rubber pad and the surface of specimen falls in a negative pressure zone. Water around the specimen is rapidly sucked into a negative pressure zone. This process exerts erosional effect on the surface of specimen.

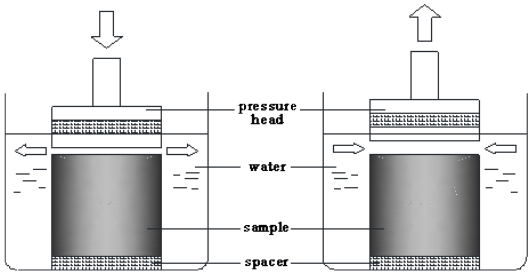

FIGURE 1. Diagram of "pump-absorb action".

(2) Cantabro Test

Good water stability and anti-loose performance are important requirements for meeting the desired pavement performance. When the fiber-reinforced stabilized soil is directly used as the surface layer of emergency airport pavement, the structural depth of the pavement may be quite deep. The fine soil aggregate of pavement surface may easily be flaked, dropped, scattered and loosened under the repeated load of airplane's wheel. This can lead to the damage on the surface of pavement, e.g., pitting. To evaluate the damaged degree of surface course caused by lack of coupling force between the soil and either the cement or fiber, the Cantabro test of FRCL was carried out in accordance with relevant method (T 0733-2011) of *Standard Test Methods of Bitumen and Bituminous Mixtures for Highway Engineering* (JTG E20-2011). The scattering loss of specimens was used to evaluate the anti-loss property of FRCL after the sample been through a certain number of rotations. At the same time, the soaked samples were used to evaluate the performance of water stability of a base-course material.

RESULTS AND DISCUSSIONS

UCS Test

By taking into account the characteristics of an emergency airfield, such as rapid construction and short-term use, this study tested the UCS (unconfined compressive strength) of samples after six different curing conditions (soaked and non-soaked for 3d, 7d and 14d). The UCS results of FRCL and cement-stabilized soil are shown in *Table III* and *Figures 2-4*.

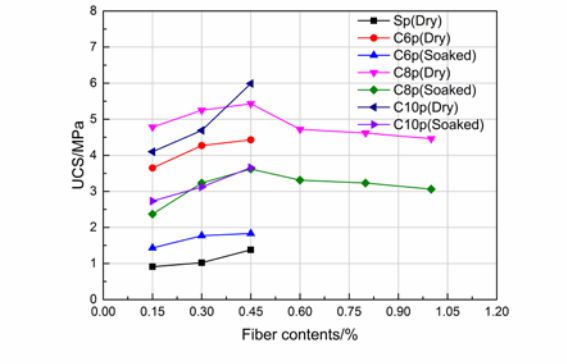

FIGURE 2. Variation of UCS with fiber content (3d).

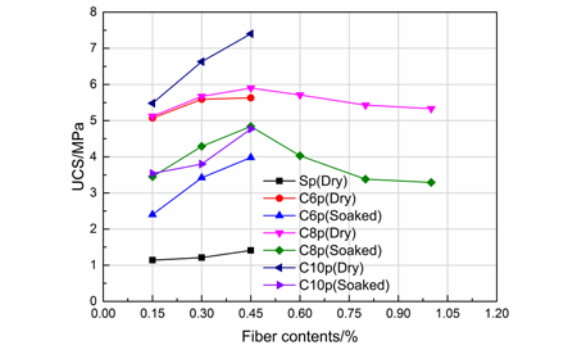

FIGURE 3. Variation of UCS with fiber content (7d).

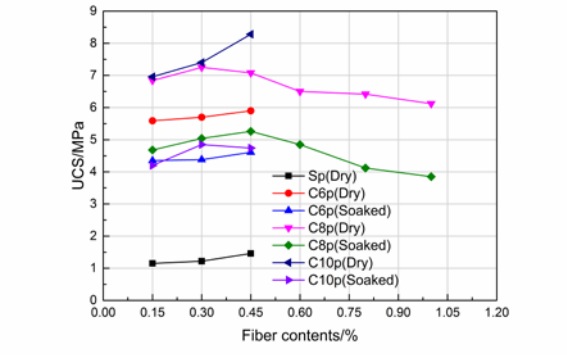

FIGURE 4. Variation of UCS with fiber content (14d).

TABLE III. Results of a UCS test.

Name of sample	3d			7d			14d		
	Dry strength , MPa	Soaked strength , MPa	Water stability coefficient, %	Dry strength , MPa	Soaked strength , MPa	Water stability coefficient, %	Dry strength , MPa	Soaked strength , MPa	Water stability coefficient, %
Sp1	0.91	-	0	1.14	-	0	1.15	-	0
Sp2	1.02	-	0	1.21	-	0	1.22	-	0
Sp3	1.38	-	0	1.41	-	0	1.46	-	0
C6p1	3.65	1.43	39.13	5.07	2.4	47.33	5.59	4.35	77.75
C6p2	4.27	1.77	41.38	5.59	3.42	61.2	5.7	4.38	76.87
C6p3	4.43	1.83	41.37	5.63	3.98	70.71	5.9	4.61	78.11
C8p1	4.78	2.37	49.49	5.12	3.45	67.4	6.84	4.68	68.41
C8p2	5.25	3.23	61.58	5.67	4.29	75.78	7.25	5.04	69.47
C8p3	5.43	3.62	66.64	5.9	4.84	82.07	7.08	5.26	74.32
C8p4	4.72	3.31	70.13	5.71	4.03	70.7	6.5	4.85	74.6
C8p5	4.62	3.23	69.95	5.43	3.38	62.34	6.42	4.12	64.15
C8p6	4.46	3.06	68.53	5.33	3.29	61.73	6.12	3.85	62.94
C10p1	4.1	2.73	66.52	5.48	3.54	64.49	6.96	4.2	60.34
C10p2	4.69	3.12	66.53	6.63	3.8	71.94	7.4	4.85	65.54
C10p3	5.99	3.66	61	7.4	4.77	51.34	8.28	4.74	57.25

Notes: The meanings of sample names are as follows: (1) initial S stands for Xi'an soil and Xs stands for Xi'an soil without any other material, C is a cement-stabilized soil prepared with Xi'an soil; (2) the middle numbers 6, 8 and 10 are the cement contents: 6%, 8% and 10% (dry soil mass percent); (3) p represents filament modified polypropylene fiber; (4) the last numbers ranged between 1 and 6 represent the fiber contents in the following order: 0.15%, 0.3%, 0.45%, 0.6%, 0.8% and 1.0% respectively. All fibers' lengths are 12 mm.

Analysis of the Influence of Cement Content

It can be observed from the inspection of *Figures 2-4* that the UCS of FRCL generally increases with the increase of cement contents. The strength of fiber-reinforced soil was kept at a low level (0.91-1.46 MPa). The water stability of the samples is poor. The strength of the sample was greatly improved after the addition of cement. The strength was much greater than that of plain soil and of fiber soil. The water stability was also improved, which was kept in the range of 40-80%. These results indicate that the addition of cement changed the nature of the soil in the FRCL samples.

Figure 5 shows the stress-stain curves of a fiber-reinforced stabilized soil at varying contents of cement. The UCS of fiber soil was greatly improved and increased with an increase in cement content. The UCS of 0.3% fiber reinforced cement stabilized samples with addition of 6% (5.13 MPa), 8% (5.51MPa) and 10% (6.66 MPa) 4.24, 4.55 and 5.5 times of the non-cement samples, respectively. The addition of cement caused the stress-strain curves of the samples to decrease rapidly after attaining the peak, indicating increasingly brittle failure.

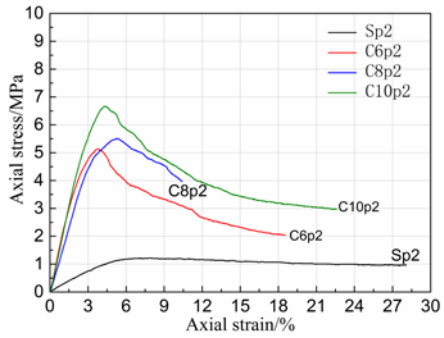

FIGURE 5. Stress-stain curves of fiber-reinforced stabilized soil for different contents of cement (7d).

Analysis of the Influence of Fiber Content

The UCS of the sample increased with an increase in fiber content. The UCS of the samples which were non-soaked and cured for 7d increased from 0.67 MPa to 1.41 MPa when the fiber contents increased from 0 to 0.45 percent. The UCS of the samples which were non-soaked and cured for 7d increased from 3.32 MPa to 7.4 MPa when the fiber contents increased from 0 to 0.45% in case of fiber-reinforced soil of C10p (refer to *Table III*).

The strength of FRCL increased two-fold over that of cement-stabilized soil (refer to *Figure 3*). The growth in strength was a result of the random distribution of fibers, which formed network structures in the soil. Due to cementation and friction between the hydration products of cement and soil particles, the fiber can effectively bear the tensile stress caused by the axial load. It can thereafter reduce the stress concentration in the specimen. The spatial distribution of the fiber-oriented network is highly dependent on the amount of fiber. A higher amount of fiber can lead to improved fiber networking. This results in improved load bearing and stress transfer. At the same time, a large number of fibers can effectively prevent the lateral deformation of the soil structure and induce certain restrictions against the sliding of the soil particles. Thus the overall mechanical properties of the specimen are improved.

The addition of fiber in the soil is significant for the construction of emergency airports in areas, where either the production of cement and lime is insufficient or transportation is difficult. It can also reduce the cost of consumption and transportation of cement. Therefore, it reduces the time of construction and facilitates the construction of emergency airports.

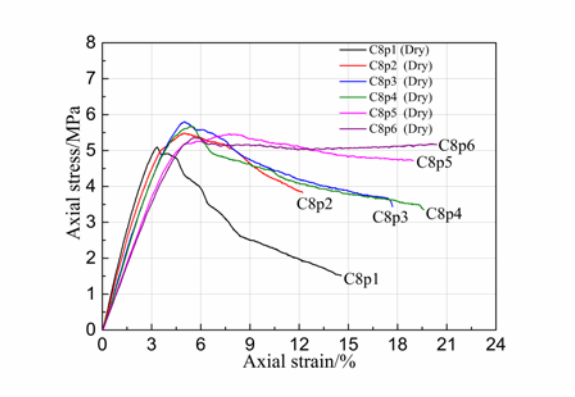

FIGURE 6. Stress-strain curves for C8p specimens (7d) [refer to *Table III*].

From the stress-stain curves of fiber-reinforced stabilized soil (refer to *Figure 5* and *Figure 6*), it can be observed that the UCS of the specimen has increased, whereas the peak stress is highly dependent on fiber content and it generally increases only with the increase of fiber content.

For all specimens stabilized by different contents of fiber and cement, the initial stress-strain curve was steep and the rate increase in stress was much higher the rate increase of strain. The results show that the addition of fiber increases the structural strength of sample at the initial stage of loading. This may reflect the strong anti-crack and reinforcement effects of the fibers. Comparing with the cement-stabilized soil and plain soil, the stress-strain curves of fiber reinforced soil had different patterns. The curve after peak descended slowly when the residual strength was at a high level. By increasing the fiber content, the curve after the peak is flat and the residual strength continued to increase. It is pertinent to note that the addition of the fiber may reduce the brittle mode of failure of the samples. The failure characteristics of the samples show a trend of transition from brittle failure toward ductility and plastic failure.

Analysis of Optimal Fiber Content

To study the effect of fiber contents on the UCS of the specimen, fibers were added to C8p at the following ratios: 0, 0.15, 0.3, 0.45, 0.6, 0.8 and 1.0 percent. It can be seen in *Figures 2-4* that the UCS of the fiber-reinforced soil first increased and then decreased with an increase of fiber contents at each age. When the fiber content was 0.3-0.45%, the UCS reached a maximum level at each age. This can be explained as follows. First, it can be inferred that additional time and mixing frequency were needed owing to the large amount of fiber in the soil. It is usually not easy to mix together the fiber and soil, and, therefore, a large amount of fiber may lead to a weak layer in the soil. In such situations, the fiber is much more likely to cause cracks under different loading conditions. Next, it can be inferred that excess fiber in the soil may reduce the random distribution of the fiber and increase the directional distribution. Since a large amount of fiber in the soil increases the chance of direct contact among fibers, the frictional force and the strength of the mixture must decrease. Therefore, in the case of an emergency airport, fiber content should be within the prescribed limits.

Anti-Erosion Test

The results of the anti-erosion test are shown in *Table IV* and *Figures 7-10*.

TABLE IV. Results of anti-erosion test.

Test method	Sample name	Erosion mass/g						Total erosion mass/g	Erosion rate /(g/min)
		5 min	10 min	15 min	20 min	25 min	30 min		
Shaking table	X6c-1	3.6	2.32	1.95	2.09	0.28	0.21	10.45	0.35
	X8c-1	1.73	1.43	1.42	0.84	1.33	0.6	7.35	0.25
	X10c-1	4.52	1.55	1.17	0.73	0.2	0.19	8.36	0.28
	C8p2-1	2.32	1.57	0.52	0.6	0.26	0.15	5.42	0.18
	C8p3-1	0.66	0.78	0.59	0.12	0.39	0.11	2.65	0.09
	C8p4-1	0.63	0.51	0.54	0.32	0.16	0.19	2.35	0.08
	C8p5-1	0.54	0.36	0.29	0.24	0.18	0.22	1.83	0.06
Fatigue testing machine	X6c-2	6.25	10.37	5.82	4.73	4.03	3.67	34.87	1.16
	X8c-2	6.81	4.98	5.09	3.67	2.53	3.3	26.38	0.88
	X10c-2	5.24	4.22	3.23	3.55	2.68	3.76	22.68	0.76
	C8p2-2	7.21	4.51	2.08	3.18	2.49	3.1	22.57	0.75
	C8p3-2	5.29	4.85	3.42	4.74	2.22	1.21	21.73	0.72
	C8p4-2	4.18	3.12	2.49	2.98	3.05	2.74	18.56	0.62
	C8p5-2	3.69	2.58	2.08	2.43	2.72	1.64	15.14	0.5

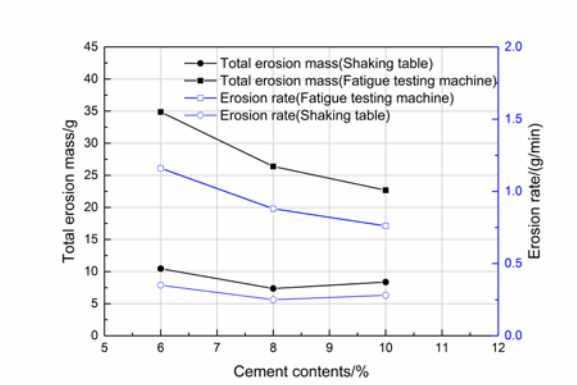

FIGURE 7. Variations in total mass of erosion and erosion rate along with cement contents.

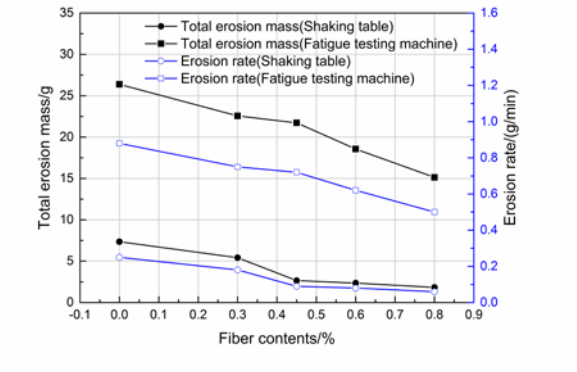

FIGURE 8. Variations in total mass of erosion and erosion rate along with fiber contents.

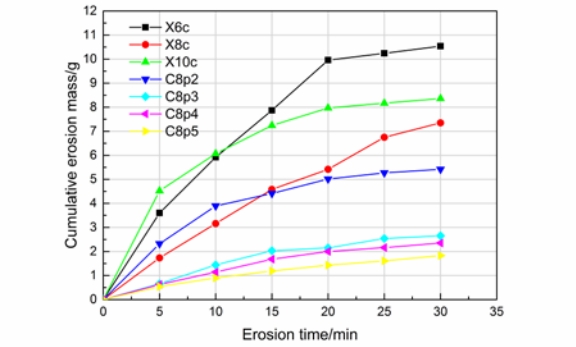

FIGURE 9. Variations of cumulative erosion mass along with erosion time, as these have been obtained by using the shaking table.

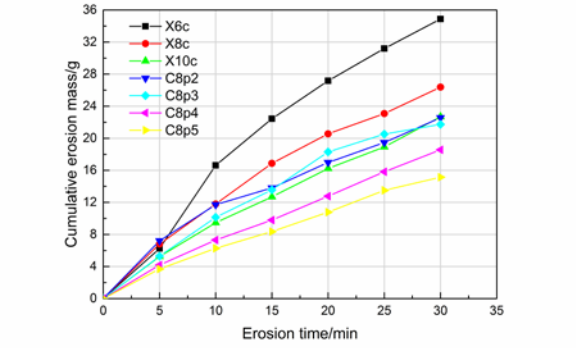

FIGURE 10. Variations of cumulative erosion mass along with erosion time, as these have been obtained by using the fatigue testing machine.

From *Table IV* and *Figures 7-10* the cumulative erosion mass of samples generally showed a linear trend of growth with increasing scouring time. The total erosion mass and erosion rate of the samples decreased with an increase in cement and fiber contents. This indicates that the anti-erosion performance has been enhanced. It can be concluded from the comparison of two experimental methods that the erosion mass and erosion rate of the shaking table method were smaller than that of the fatigue testing machine. For example, when the erosion time was 30 min, the erosion mass recorded by the shaking table method ranged between 1.83-10.45 g, whereas the erosion rate ranged between 0.06-0.35 g/min. At an erosion time of 30 min, the erosion mass as recorded by fatigue testing machine method ranged between 15.14-34.87 g, whereas the erosion rate ranged between 0.50-1.16 g/min. This is a result of the testing process of shaking table method. There were only the "pump-absorb action" and the dynamic water pressure without any loading impact, which led to a slower erosion process.

It can be inferred from *Figure 9* and *Figure 10* that during the testing process of shaking table method, the initial erosion rate of sample was large. The slope of the curve was significantly decreased and the erosion mass of the sample gradually slowed down and tended to be stabilized over time. In the case of the fatigue testing machine method, the initial erosion mass of sample was large but the mass of erosion increased and the accumulative erosion mass and erosion time were approximately linear with time.

Comparing the anti-erosion properties of FRCL and cement-stabilized soil tested using the two different anti-erosion test methods, the erosion mass and erosion rate of FRCL that were less than that of cement-stabilized soil. The anti-erosion performance of stabilized soil increased approximately 26-75% after the addition of fiber. This indicates the effect of fiber on anti-erosion performance of stabilized soil was very significant. By combining the analyses of UCS test results in section 2.1, it is noted that there is a definite correlation between the anti-erosion performance of the material and the compressive strength. It is pertinent to note that the improvement in compressive strength of soil block (combined soil) resulted in improvement in anti-erosion performance. This was due to the fiber-reinforced compressive strength of the material. The bond strength between the particles of the soil was improved to a certain extent. This also enhanced the anti-erosion performance of the material.

Cantabro Test

The results of the Cantabro test are shown in *Table V*, *Figure 11* and *Figure 12*. From *Table V* and *Figure 11*, the curves of variations for the residual mass of dry samples along with the rotation number can be divided into three stages. These three stages are the initial stage, the rapid scattering stage and the stable stage. In the initial stage, samples exhibit good integrity and low scattering loss. Most scattering losses were caused by loose particles on the surface of the specimen and at the edge of the circumferential surface. For plain soil and cement-stabilized soil, this initial stage contained 0-40 turns. In case of FRCL, the duration of initial stage was longer and it contained 0-80 (100) turns. In the rapid scattering stage internal damage and sample cracks developed and expanded rapidly. This stage appeared earlier in the case of low cement content, where scattering loss reached up to 60-80%. In the third stage, the remaining part of the specimen was always hard, therefore, the scattering loss tended to be stable.

TABLE V. Results of Cantabro test.

Curing methods	Sample name	Mass before test/g	Mass after test/g	Scattering loss/%
Curing 7 days, dry	Xs-1	1147.24	64.82	94.35
	X6c-1	1138.85	389.42	65.81
	X8c-1	1170.84	521.65	55.45
	X10c -2	1162.94	590.78	49.2
	C8p2-2	1119.2	971.54	13.19
	C8p3-2	1113.06	959.82	13.77
	C8p4-2	1092.82	744.21	31.9
	C8p5-2	1080.04	652.58	39.58
Curing 7 days, soaking	X6c-2	1136.7	290.37	74.46
	X8c-2	1138.22	455.99	59.94
	X10c-1	1139.15	561.35	50.72
	C8p2-1	1142.21	581.65	49.08
	C8p3-1	1132.26	800.29	29.32
	C8p4-1	1124.59	558.88	50.3
	C8p5-1	1106.55	610	44.87

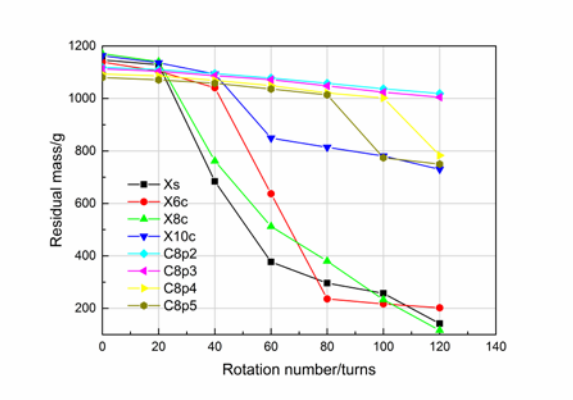

FIGURE 11. Variations of residual mass of dry samples along with rotation numbers.

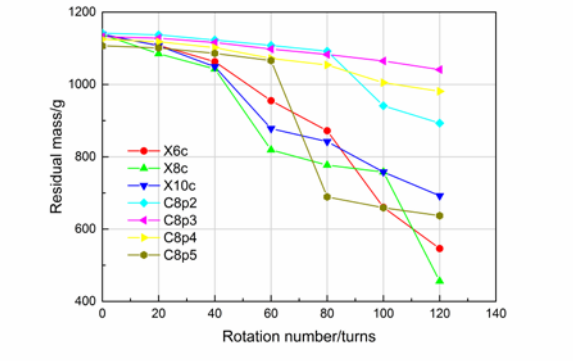

FIGURE 12. Variations of residual mass of soaked samples along with rotation numbers.

From *Figure 12*, as revolutions increase, the remaining mass of soaked samples constantly decreases, whereas the rate of scattering loss fluctuated within a certain range. The rate of scattering loss of soaked samples was larger than that of non-soaked samples. The results indicate that the absorbed water penetrated into the interior of the material and the softening effect of water reduced the cohesion of the matrix and the bond strength decreased. Therefore, the soaked samples showed greater scattering loss. The scattering loss of soaked and non-soaked samples decreased with an increase in cement content. This indicates that the anti-scattering and anti-loose characteristics of the samples are sensitive cement content. It is pertinent to mention that the anti-loose performance of the cement-stabilized soil increased rapidly as the cement content increased.

The scattering rate of soaked and non-soaked samples first decreased and thereafter increased with an increase of fiber content. When the fiber content was 0.45%, the samples of fiber-reinforced soil exhibited a minimum rate of scattering loss and the best anti-scattering performance. The performance of the FRCL gradually reduced when the cement content increased. Owing to the increased fiber contents, the uniformity of the fiber in the sample decreased. A large amount of fiber in the soil led to the formation of a weak layer, resulting in increased the scattering loss during the test. At optimum loading, the fiber is distributed uniformly and can form a three-dimensional space-staggered distribution. The fiber can better connect the soil particles, and the integrity of the specimen is improved.

ANALYSIS OF EROSION MECHANISM AND SCATTERING MORPHOLOGY

Erosion Mechanism of Cement-Stabilized Material

Figure 13 shows the process of erosion failure of fiber-reinforced stabilized soil. The mechanism of anti-erosion performance of cement-stabilized soil and FRCL is discussed in the following paragraph. This based on the process of erosion failure, as shown in *Figure 13*.

The mechanism of anti-erosion performance of cement-stabilized soil consists mainly of three aspects: (1) the cement particles were uniformly dispersed in the soil and the cement stone skeleton was formed under the action of hydration and compaction during the construction process of airport pavement when the cement was added in soil, (2) the micro-structure of the cement stone skeleton on the surface of the base course was first destroyed under the dual effects of the wheel load and hydrodynamic water pressure when the base course material was eroded, and (3) the soil particles and damaged debris may be washed away during the combined effects of "pump suction", high speed water flow and hydrodynamic water impact force without the support and protection of the cement stone skeleton. Cement content had a significant effect on the formation of cement stone skeleton, so the addition of cement content had a great influence on the anti-erosion performance of fiber-stabilized soil. The anti-erosion performance of the cement-stabilized soil increased with an increase in cement content.

(a) 0 min (b) 5 min (c) 10 min (d) 15 min

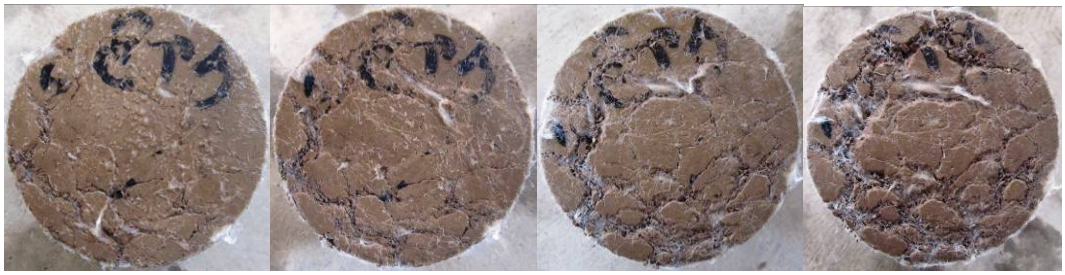

(e) 20 min (f) 25 min (g) 30 min (h) 35 min

FIGURE 13. Erosion failure process of fiber-reinforced stabilized soil (C8p5-2).

The mechanism of anti-erosion performance of FRCL consists mainly of the following aspects. The addition of the fiber significantly enhanced the anti-cracking and anti-fatigue properties as well as toughness of the material, which reduced the cracks greatly and improved the stability and continuity of the stabilized soil. The addition of fiber also effectively prevented water penetrating into the specimen, and improved the anti-erosion performance. The modified polypropylene fiber had good dispersion, high modulus and tensile strength. When the fiber was mixed into cement-stabilized soil, the fiber was wrapped into a cement paste and was distributed among soil particles in a three-dimensional, random direction. The bonding force between the fiber and the cemented material formed a supporting composite system in three-dimensional network space. It improved the integrity of particles on the surface of the base course, which reduced the dynamic water scouring force on the particles of weak layer in the base course. The erosion of loose soil particles and the anti-erosion performance of the material were further enhanced [19-20].

The Surface Morphology Analysis of Scattering Failure Sample

Figures 14-17 show the scattering failure process of soil sample, stabilized soil sample and reinforced soil sample.

(a) 0 turn (b) 20 turns (c) 40 turns (d) 80 turns (e) 160 turns

FIGURE 14. Scattering failure process of soil sample (Xs).

(a) 0 turn (b) 20 turns (c) 40 turns (d) 80 turns (e) 160 turns

FIGURE 15. Scattering failure process of cement-stabilized soil sample (X10c-2).

(a) 0 turn (b) 20 turns (c) 40 turns (d) 80 turns (e) 160 turns

FIGURE 16. Scattering failure process of fiber-reinforced stabilized soil sample (C8p2-2).

(a) 0% (X8c) (b) 0.3% (C8p2) (c) 0.45% (C8p3) (d) 0.6% (C8p4) (e) 0.8% (C8p5)

FIGURE 17. Scattering failure process of a soil sample that has been reinforced by different contents of fiber.

The samples photos in *Figures 14-17* basically confirm the earlier discussion regarding the three stage scattering process (section 2.3) In the initial stage, scattering damage occurred only in the two end edges of sample. In the second stage, the soil sample was rapidly decomposed; there were two or more blocks of the same size in the scattering residue after several turns. In the case of a cement-stabilized soil sample, the hydration

reaction product created a strong bond. The residual mass was about half of the original quality after 160 turns. In the case of a FRCL sample, the anti-scattering ability is greatly enhanced, and the scattering loss was very small. The specimen remained intact after 160 turns with small damage in the two end edges.

Figure 17 shows that the scattering process of sample failure changed as a function of fiber content. It can be observed that the sample without fiber addition was divided into numerous small pieces after test, and there was a large amount of scattering residue, essentially blocks. However, the sample reinforced by fiber remained intact after the test. The scattering residues were large and most of the damage happened on the surface of the specimen and on edge of the circumferential surface. The scattered material did not look like the block, but like the soil particles. It can be found from the comparison of the morphology the damaged samples that the anti-scattering ability decreased with increasing fiber content. The uniformity of the fiber in the sample decreased when too much fiber is added. Too large an amount of fiber led to the

formation of a weak layer in the soil mass and increased the scattering loss. This is in alignment with the statement in section 2.3 that there is an optimum content of fiber associated with the anti-scattering performance of FRCL.

CONCLUSION

On the basis of the experiments and resulting data, the following conclusions are possible:

The dual effects of chemical strengthening caused by hydration of cement and physical reinforcement (anchorage reinforcement) of fiber greatly improved the unconfined compressive strength (UCS) and water stability of the specimen. The water stability fell in a range of 40-80 percent. As cement and fiber contents increased within a certain range, the UCS of the sample continuously improved. The addition of cement made the stress-strain curves of the samples decrease rapidly after the peak and begin to show the characteristics of brittle failure. The addition of fiber increased the strength of the samples, while decreasing the tendency toward brittle failure. The optimum fiber content was found to be in the range of 0.3-0.45 percent.

The cumulative erosion mass of samples generally showed a linear trend of growth as a function of scouring time. The total erosion mass and erosion rate of samples decreased as cement and fiber contents increased, whereas the anti-erosion performance of stabilized soil increased by 26~75% after the addition of fiber. This indicates that the effect of fiber on anti-erosion performance of stabilized soil is very significant. By comparing the test methods of shaking table and fatigue testing machine, the erosion effect of later method was more obvious. A certain correlation exists between the anti-erosion performance of the material and its compressive strength. The improvement of compressive strength resulted in improvement of its anti-erosion performance.

The scattering process of samples can be divided into the following three stages: (i) the most scattering loss was caused by loose particles on the surface of the specimen as well as on the edge of the circumferential surface. For the case of plain soil and cement-stabilized soil, this stage contained 0-40 turns, whereas for FRCL, this stage contained 0-80 (100) turns; (ii) the rapid scattering stage often appeared early for samples low in cement content and the scattering loss may reach up to 60-80%; and (iii) the scattering loss tended to be stable in the third stage. With an increase of fiber content, the anti-scattering properties of samples first increased and then decreased. It is pertinent to note that 0.45% was the optimum content of fiber and this was consistent with the results of UCS test.

REFERENCES

[1] Anderton, G. L., Berney, I. V., Ernest, S., Mann, T. A., Newman, J. K., Baylot, E. A., & Mason, Q. (2008). *Joint rapid airfield construction (JRAC) 2007 technology demonstration* (No. ERDC/GSL -TR-08-17). ENGINEER RESEARCH AND DEVELOPMENT CENTER VICKSBURG MS GEOTECHNICAL AND STRUCTURES LAB.

[2] Sharma, V., Vinayak, H. K., & Marwaha, B. M. (2015). Enhancing compressive strength of soil using natural fibers. *Construction and Building Materials*, *93*, 943-949.

[3] Hejazi, S. M., Sheikhzadeh, M., Abtahi, S. M., & Zadhoush, A. (2012). A simple review of soil reinforcement by using natural and synthetic fibers. *Construction and Building Materials*, *30*, 100-116.

[4] Divya, P.V, Viswanadham, B.V.S, & Gourc, J.P. (2014). Evaluation of tensile strength-strain characteristics of fiber-reinforced soil through laboratory tests. *Journal of Materials in Civil Engineering*, *26*(1), 14-23.

[5] Lecompte, T., Perrot, A., Subrianto, A., Le Duigou, A., & Ausias, G. (2015). A novel pull-out device used to study the influence of pressure during processing of cement-based material reinforced with coir. *Construction and Building Materials*, *78*, 224-233.

[6] Tang, C. S., Shi, B., & Zhao, L. Z. (2010). Interfacial shear strength of fiber reinforced soil. *Geotextiles and Geomembranes*, *28*(1), 54-62.

[7] Zhu, H. H., Zhang, C. C., Tang, C. S., Shi, B., & Wang, B. J. (2014). Modeling the pullout behavior of short fiber in reinforced soil. *Geotextiles and Geomembranes*, *42*(4), 329-338.

[8] Alrashidi MJK, & Alrashidi M. (2006). Durability and mechanistic characteristics of fiber reinforced soil-cement mixtures. *The International Journal of Pavement Engineering*, *7*, 53-62.

[9] Danso, H., Martinson, D. B., Ali, M., & Williams, J. (2015). Effect of fibre aspect ratio on mechanical properties of soil building blocks. *Construction and Building Materials*, *83*, 314-319.

[10] Park, S. S. (2011). Unconfined compressive strength and ductility of fiber-reinforced cemented sand. *Construction and Building Materials*, *25*, 1134-1138.

[11] Tang, C. S., Wang, D. Y., Cui, Y. J., Shi, B., & Li, J. (2016). Tensile strength of fiber reinforced soil. *Journal of Materials in Civil Engineering*, *28*(7).

[12] Akbulut S, Arasan S, & Kalkan E. (2007). Modification of clayey soils using scrap tire rubber and synthetic fibers. *Applied Clay Science*, *38*, 23-32.

[13] Punthutaecha K, Puppala A J, & Vanapalli S K. (2006). Volume change behaviors of expansive soils stabilized with recycled ashes and fibers. *Journal of Materials in Civil Engineering*, *18*, 295-306.

[14] Mohamed, A. E. M. K. (2013). Improvement of swelling clay properties using hay fibers. *Construction and Building Materials*, *38*, 242-247.

[15] Kumar A, Walia BS, & Bajaj A. (2007). Influence of fly ash, lime, and polyester fibers on compaction and strength properties of expansive soil. *Journal of Materials in Civil Engineering*, *19*, 242-248.

[16] Kumar A, Walia BS, & Mohan J. (2006). Compressive strength of fiber reinforced highly compressible clay. *Construction and Building Materials*, *20*, 1063-1068.

[17] Ibraim, E., Diambra, A., Russell, A. R., & Wood, D. M. (2012). Assessment of laboratory sample preparation for fibre reinforced sands. *Geotextiles and Geomembranes*, *34*, 69-79.

[18] VAN WIJK A J. (1985). Rigid pavement pumping: (1) Subbase erosion and (2) Economic modeling. West Lafayette, Purdue University.

[19] Sha, A. M., & Hu, L. Q. (2002). Study of testing method for anti-erosion properties of semi-rigid base materials. *China Journal of Highway and Transport*, *15*(2), 4-7.

[20] Sha, A. M., Hu, L. Q. (2002). Experimental study on the anti-erosion properties of pavement base materials. *Chinese Journal of Geotechnical Engineering*, *24*(3), 276-280.

[21] Zhu, T. L., Tan, Z. M., & Zhou, Y. M. (2013). Experimental research on erosion-resistance performance of semi-rigid base materials. *Journal of Building Materials*, *16*(4), 608-613.

[22] Caro, S., Caicedo, B., Varela, D., Monroy, J., Wills, J., Hernandez, M. A., & Beltran, D. (2015, June). Experimental Evaluation of Erosion Processes in Rigid Pavements. In *Airfield and Highway Pavements 2015* (pp. 512-523).

AUTHORS' ADDRESSES

Jun Zhang
Xing-Zhong Weng
Jun-Zhong Liu
Air Force Engineering University
No. 1 Ba Ling Road, Baqiao District
Xi'an, Shaanxi 710038
CHINA